Proceedings of the ASME 2022
Internal Combustion Engine Division Fall Technical Conference
ICEF2022
October 16-19, 2022, Indianapolis, Indiana

ICEF2022-XXXXX

SIMULATION OF SPRAY, WALL-FILM, AND CHARGE PREPARATION FOR LIGHT-DUTY, COLD-START APPLICATIONS

K. Dean Edwards
Oak Ridge National Laboratory
Oak Ridge, TN USA

ABSTRACT

For modern, light-duty engine applications, the development of improved operating strategies to expedite catalyst heating during cold-start operation is essential for further reduction of emissions and meeting of future regulations. The development of such strategies would benefit from numerical modeling tools capable of accurate prediction of charge preparation, combustion, and emissions formation at cold-start conditions. Traditional development of simulation tools has primarily focused on standard engine operating conditions, and, as a result, these tools have difficulty accurately capturing extreme behavior during cold-start operation such as extensive wall wetting due to fuel-spray impingement on cold cylinder surfaces, late combustion phasing to increase exhaust enthalpy, and continued oxidation of reactants in the exhaust system. A major objective of the multi-national-laboratory Partnership to Advance Combustion Engines (PACE) consortium is the development and evaluation of new modeling approaches for cold-start operation. In this paper, we present recent progress in simulating charge preparation in a light-duty, multi-cylinder, gasoline engine during cold-start relevant conditions as defined by the U.S. DRIVE Advanced Combustion and Emission Control (ACEC) Tech Team cold-start protocols for catalyst heating. We focus study on fuel spray and spray–wall interactions resulting in extensive film formation due to cold cylinder walls. Simulation results are evaluated at steady-state, cold-start relevant operating conditions. Predictions for film formation and composition with conventional (baseline) models are compared to results with new simulation tools and approaches developed under PACE including the Corrective Distortion Spray Model developed by Sandia National Laboratories, which accounts for non-spherical droplet shapes, and a new spray–wall interaction model developed by Argonne National Laboratory, which accounts for multi-droplet, non-uniform impingement. The current study expands on past studies validating these new submodels with spray-chamber experimental measurements to examine the impact they have on full engine CFD simulations.

Keywords: Cold start, spray–wall interaction, PACE

NOMENCLATURE[1]

ACEC	U.S. DRIVE Advanced Combustion and Emissions Control
CAD	crank angle degree
CD	Corrected Distortion spray model
CFD	computational fluid dynamics
CHT	conjugate heat transfer
CT	computerized tomography
dATDC	degrees after top dead center
DOE	U.S. Department of Energy
ICE	internal combustion engine
nIMEP	net indicated mean effective pressure
NTC	No Time Counter collision model
PACE	Partnership to Advance Combustion Engines
RANS	Reynolds-Averaged Navier–Stokes
SOI	start of injection
SWI	spray–wall interaction model

1. INTRODUCTION

The overall goal of DOE's Partnership to Advance Combustion Engines (PACE) consortium is to develop improved predictive simulations tools to aid efforts to overcome key barriers to improved efficiency and reduction of carbon and pollutant emissions in internal combustion engines (ICEs) during the proposed transition to an electrified light-duty market. Among those barriers is the need for improved simulation accuracy during cold-start operation and warming of the catalytic converter when the majority of pollutant emissions are released in modern gasoline vehicles [1]. Cold-start operation presents many challenges for accurate prediction of charge preparation, combustion, and emissions production using conventional simulation approaches designed and calibrated for normal engine operation. During fuel injection into the cold cylinder environment, evaporation is limited, allowing deep penetration of the liquid fuel and increased wall wetting, film formation, and fuel pooling. To accurately simulate charge preparation and in-cylinder conditions as well as production of soot due to combustion of liquid fuel on the combustion chamber surfaces, models must be able to accurately predict the formation and evolution of wall films. For warm engine operation, wall wetting is a minor concern; therefore, little effort has been focused on improving spray–wall interaction submodels in recent years. The modeling approach most commonly used for ICE fuel spray interactions with combustion chamber surfaces was developed by O'Rourke and Amsden in 2000 [2] and is based on studies of single-droplet impacts [3].

As part of the PACE consortium efforts, new submodels [4–5] have been developed and integrated for use in CFD simulations to improve predictive accuracy of fuel spray, evaporation, and spray–wall interactions in ICEs. The purpose of this study is to integrate those new tools into a CFD engine simulation for cold-start operation and compare predictions of wall-film formation and charge preparation.

2. MATERIALS AND METHODS

The CFD engine model used for this study is based on a GM 2-L Ecotec LNF engine and was created using the commercial CFD code CONVERGE v3.0 [6]. Engine geometry was obtained from CT and laser scans of purchased production hardware. Intake and exhaust manifolds match those of an experimental engine setup at ORNL that was converted for single-cylinder operation. Valve timings and lift profiles were physically measured at ORNL by manually spinning the engine and measuring valve lift. Information for the stock 6-hole, axisymmetric injector was obtained from physical measurements and limited spray-chamber experimental measurements conducted at ambient conditions by Sandia National Laboratories.

The baseline modeling approach uses conventional settings and submodels typical for CFD simulation of direct-injection, gasoline engines. A 2-mm cubic base grid was used with additional refinement to 0.5 mm in the fuel spray and along the combustion chamber surfaces. Adaptive mesh refinement was applied to 0.5 mm for subgrid gradients in velocity (>5 m/s) and temperature (>10 K). Turbulence was modeled with a Reynolds-Averaged Navier–Stokes (RANS) k–ε model.

Simulations in this study used a nine-component liquid fuel surrogate based on RD5-87 research gasoline and developed by the PACE consortium's Fuel Team. The surrogate formulation was developed to match multiple fuel properties and performance metrics including the boiling curve, octane numbers and sensitivity, φ sensitivity, and sooting propensity. Composition of the surrogate is presented below in Table 1.

Fuel spray was modeled using a Lagrangian–Eulerian approach with Lagrangian-tracked fuel parcels passing through a Eulerian reference system. Physical measurements of the stock injector and imaging from the limited spray-chamber experiments preformed at Sandia National Laboratories were used to set injector geometry and tune spray model parameters including cone angle. In absence of spray-rate profile measurements, a trapezoidal profile was assumed. Injector discharge coefficient was determined based on experimental data for injected mass, injection duration, and injector pressure at the target engine operating point.

For the baseline model, submodels and settings were chosen from available options within CONVERGE based on accepted best practices for modeling direct-injection gasoline engines. The fuel spray was modeled with an initial "blob" distribution, Kelvin–Helmholtz and Rayleigh–Taylor (KH–RT) breakup models, and the No Time Counter (NTC) collision model as implemented in CONVERGE v3.0 [6]. Droplet drag assumed spherical droplets. Liquid fuel components were set to evaporate to their equivalent gaseous species based on the Frössling droplet evaporation model for parcels and a uniform-temperature approach for the film [6]. An adaptive film mesh with two embedding levels was used to reduce grid-alignment errors in determining film thickness [6].

The current study is focused on comparing predictions of film formation and evolution in a light-duty gasoline engine at cold start–relevant conditions using the baseline model and integrating new submodels for free spray and spray/wall interactions developed by the PACE consortium Spray Team. The new submodels were introduced in stages to track their individual contributions to any improved performance.

For the first stage of submodel integration, a flash boiling model [7] implemented into CONVERGE v3.0 was activated with default settings [6]. At the cold start–relevant conditions of this study, the addition of this model had little impact with no flash boiling of lighter, more volatile species predicted.

Next, the Corrected Distortion (CD) spray model [4], developed by Sandia National Laboratories under the PACE consortium and implemented as a hidden feature in CONVERGE v3.0, was activated. This model refines the treatment of droplet drag and evaporation in the free spray by accounting for non-spherical droplet shapes. A more detailed description of the model can be found in [4].

The final submodel included in the integrated model is a new spray–wall interaction (SWI) model [5] developed at Argonne National Laboratory under the PACE consortium and implemented into CONVERGE v3.0 as a user-defined function.

This submodel seeks to improve upon the classic O'Rourke–Amsden SWI model [2] by accounting for impingement of multiple, irregularly timed and spaced droplets based on work by Stanton and Rutland [8–10]. Depending on the balance of surface tension forces and droplet inertia, a fuel droplet impacting the wall is considered to either stick to the wall as a film, rebound off the wall, or "splash" with some liquid joining the film and some bouncing off. In the O'Rourke–Amsden model, collision outcomes are decided based on the Weber number of the droplet and a non-dimensional splashing parameter, E^2, which depends upon the existing film thickness at the point of impact and the droplet's diameter and Reynold's number [2,6]. A new splashing criterion, $We_{o,splash}$, is introduced in the Argonne SWI model which adds accounting for the frequency of droplet impacts [5]. The Argonne SWI model also tracks the inertia of liquid as it forms (or joins) the film allowing it to spread away from the impact site as opposed to the O'Rourke–Amsden model which assumes that liquid which sticks to the wall loses its momentum upon impact [2]. Comparisons between simulations with the SWI model and spray-chamber experimental measurements have shown improved agreement over the conventional models for gasoline boiling-range fuels [5]. In addition to spray–wall interactions, CONVERGE also includes a film-separation model which accounts for film parcels being convected from edges of the wall surface [6].

Operating conditions for the study were based on the U.S. DRIVE ACEC Tech Team Cold-start Protocols for catalyst heating with steady-state operation at 1300 rpm and 2-bar nIMEP with intake air, engine coolant, and oil maintained at 20°C. Spark timing was delayed to sweep exhaust enthalpy for accelerated catalyst heating. This approach required increased fueling and reduced throttling to maintain the target load and stoichiometry over the enthalpy sweep. Because the current study is focused on wall-film formation, spark and chemistry were turned off in the model while maintaining fuel injection rates (~16 mg/inj) and intake pressure (~0.5 bar) for a point roughly midway through the exhaust enthalpy sweep described above.

In-cylinder thermal boundary conditions were set based on separate CFD simulations for fired operation at the same conditions under the ACEC Tech Team Cold-start Protocols using a coupled 3-D conjugate heat transfer (CHT) model of the engine. Based on CHT model results, which showed little spatial variability for cylinder components except for the head, constant and uniform wall temperatures were applied to cylinder components as follows: liner, 25°C; piston, 50°C; head and intake valve, 80°C; exhaust valve, 140°C. While the CHT model predicted approximately 40°C temperature gradient across the head, a uniform average head temperature was used during this study for simplicity.

A single injection during intake at −280 dATDC was chosen because this set of conditions produces substantial wall film. The single injection strategy also provides simplicity for the study by eliminating multiple injection effects allowing clearer focus on spray–wall collision outcomes and spray evolution during compression.

3. RESULTS AND DISCUSSION

Figure 1 shows total predicted fuel mass at the test condition for the four model approaches. At these conditions, roughly 1/3 of the injected fuel mass initially forms a film on cylinder surfaces with limited evaporation during the intake and compression strokes leaving about 16% of the injected fuel in the wall film during the spark timing window (±30 dATDC). Significant differences in predicted total film mass are only noted when the new SWI model is included resulting in a small increase in initial film formed. However, the additional film mass dissipates quickly during the remainder of the intake stroke with all four models converging to a similar total film mass at top dead center.

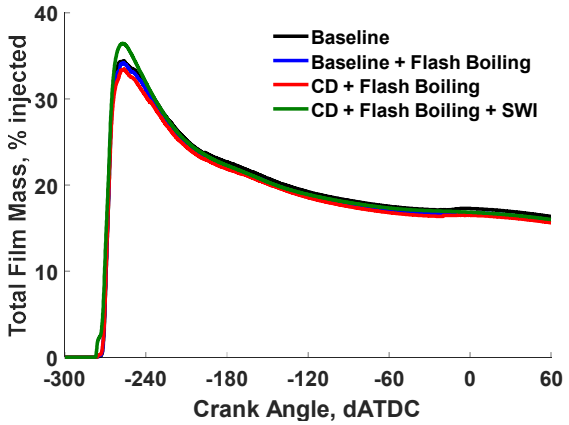

FIGURE 1: Percent of injected fuel mass in total wall film predicted by four modeling approaches.

The baseline and integrated models also predict similar mass-averaged film compositions as shown in Figure 2. No flash boiling of the lighter species is noted to occur at these conditions, but preferential evaporation of the lighter species results in a film composition that differs significantly from the PACE-20 formulation as shown in Table 1. Only a small amount of the lighter species reaches the wall, and that which does evaporates quickly and (almost) completely from the film during the remainder of the intake stroke. A larger percentage of the heavier species reaches the walls with most remaining through intake and compression. Note that the results presented here are mass-based averages over the total film mass. Further analysis (not included here for brevity) also shows significant spatial variation in film composition throughout the cylinder.

Despite the limited differences observed in total film mass and composition for the two models, there are differences in the predicted location of film formation and the outcomes of wall impacts. Figure 3 shows that the integrated model predicts more film forming on the piston and liner and less on the head. Unlike the initial differences in total film mass discussed above, these differences persist through intake and compression.

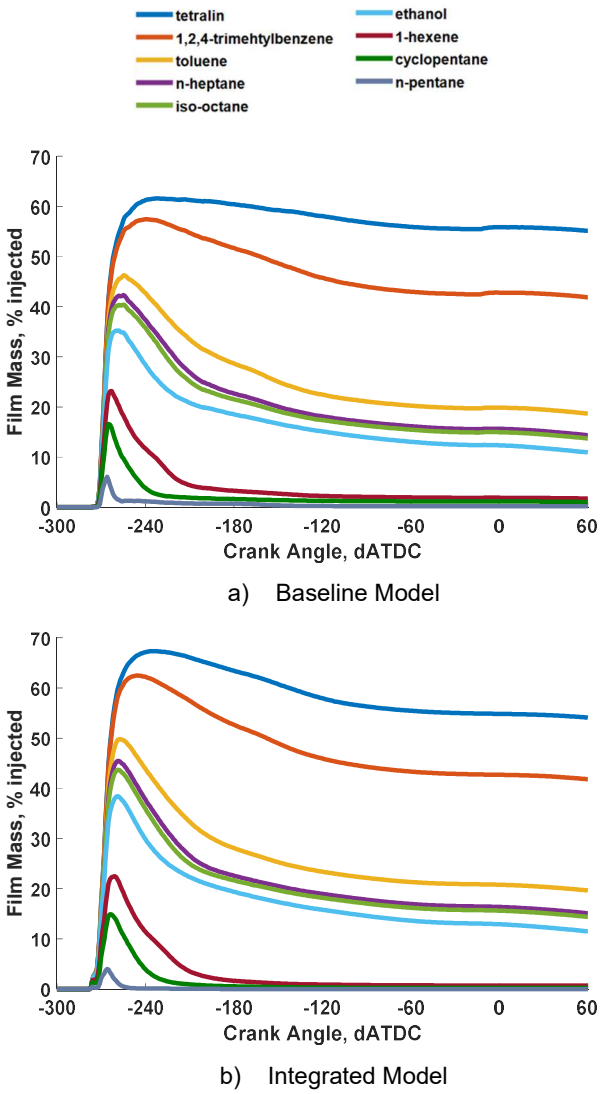

FIGURE 2: Percent of injected fuel mass for each surrogate component in total wall film predicted by two modeling approaches.

TABLE 1: Comparison of PACE-20 surrogate composition to film composition at top-dead-center (TDC) predicted with the integrated model. Red and blue text highlights significant increases and reductions, respectively, in species concentration within the film relative to the PACE surrogate formulation.

	Mass Fraction, %	
	PACE-20	Film @ TDC
ethanol	10.16	7.68
n-pentane	11.68	0
1-hexene	4.91	0.20
toluene	10.79	13.13
n-heptane	10.63	10.18
iso-octane	23.41	21.42
1,2,4-trimethylbenzene	13.96	34.91
cyclopentane	10.62	0.14
tetralin	3.84	12.33

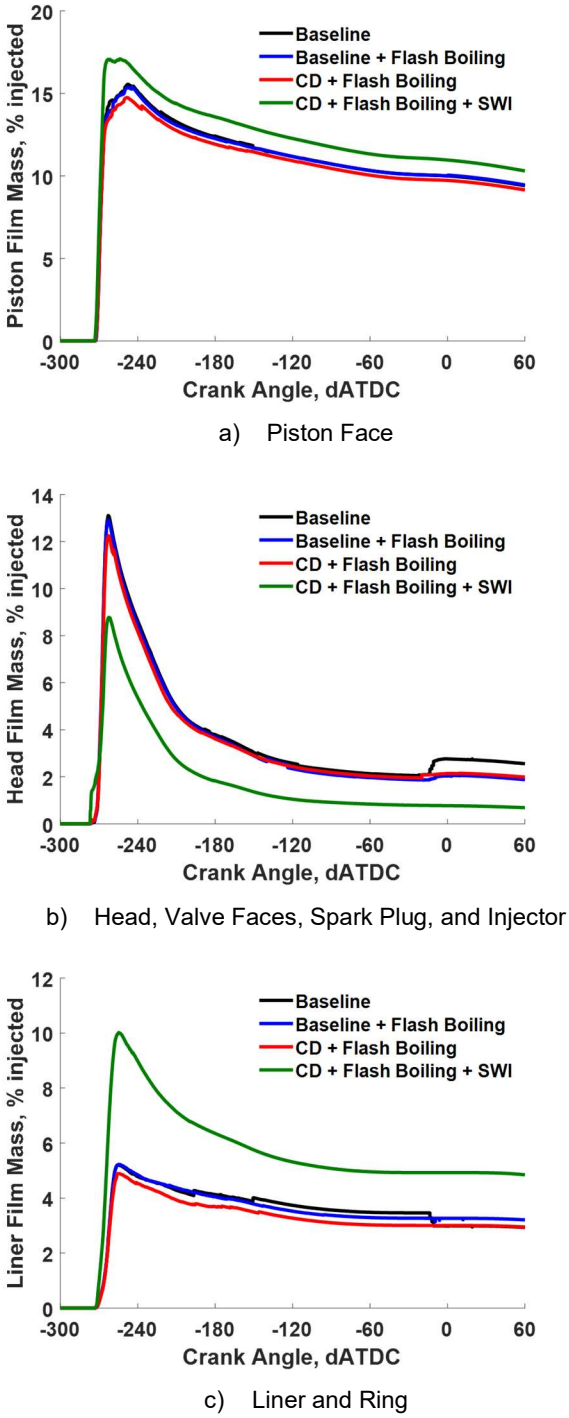

FIGURE 3: Percent of injected fuel mass in film formed on cylinder surfaces predicted by four modeling approaches.

The LNF stock injector has a 6-hole, axisymmetric spray pattern. Figure 4 isolates spray patterns for the 3 nozzles on one side of the injector 10 CAD after start of injection. Spray from Nozzle 1 proceeds unimpeded to impact the piston cup. At this injection timing, plumes from nozzles 2 and 3 clip the intake

valve disrupting a portion of the spray while the remainder continues across the cylinder eventually impacting the liner.

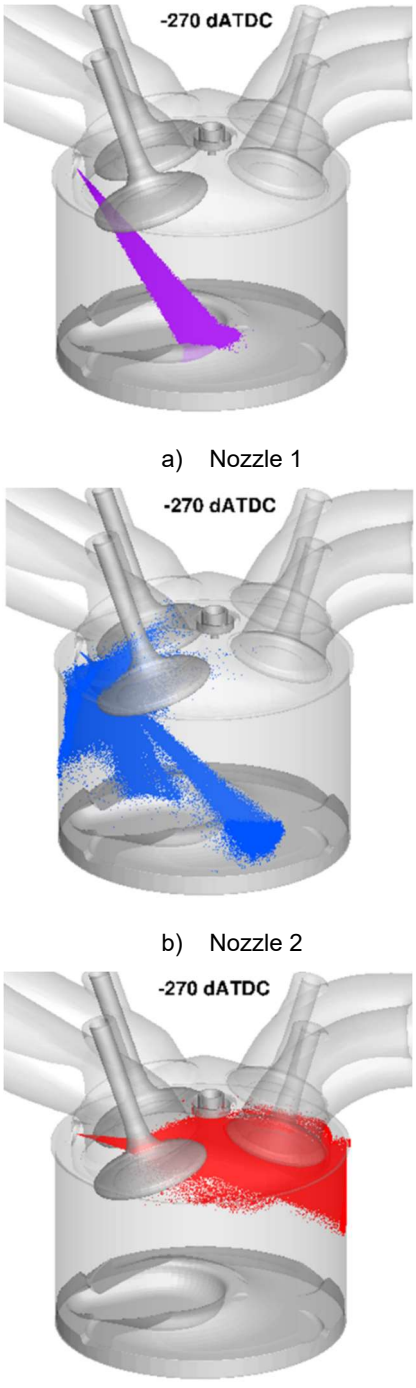

FIGURE 4: Predicted spray distribution for each injector nozzle (remaining 3 nozzles are axisymmetric) 10 CAD after start of injection using the integrated model.

Figures 5 and 6 compile the mass of the fuel parcels based on the outcomes of parcel–wall collisions predicted by the baseline and integrated models. Figure 5 compiles the total fuel mass for all injector nozzles, and Figure 6 compiles the fuel mass for each of the three injector nozzles shown in Figure 4. As discussed above and shown again in Figure 5, the integrated model predicts a slightly higher initial film mass, however there are substantial differences in predicted outcomes of wall collisions. Overall, the integrated model predicts less splashing and rebound but a substantial increase in film separation.

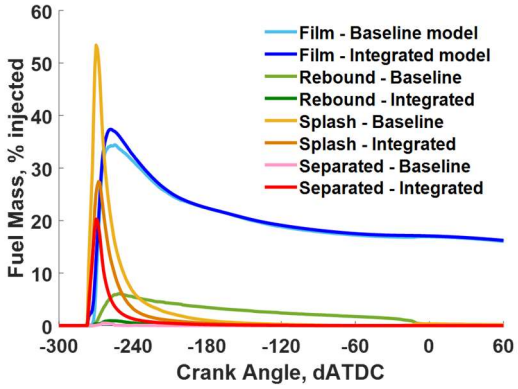

FIGURE 5: Percent of total injected fuel mass grouped by outcome of wall collision predicted by two modeling approaches.

The distributions for Weber number, diameter, and velocity of free parcels prior to impact are similar for both models so the differences appear to be due to differences in the collision outcome criteria for each model. Information used by the models to determine the outcome of individual spray–wall collisions (e.g., E^2, $We_{o,splash}$) is not available in the CONVERGE output making it difficult to fully explore the specific differences for a given collision. However, some information can be gleaned by comparing the results in Figure 6 with 3-D visualizations of the parcel distributions grouped by predicted outcome as shown in Figure 7. In these plots, taken 10 CAD after start of injection, film parcels are shown in blue, rebound parcels in green, splash parcels in yellow, and separated parcels in red.

For Nozzle 1, about half of the injected fuel forms film on the piston with most of the rest splashing off. The integrated model predicts more film formation and less splashing from the impact of Nozzle 1 plume on the piston than the baseline model. The integrated model also predicts less rebound but slightly higher separation than the baseline model.

For Nozzle 2 the baseline model predicts that the majority of the injected fuel spray splashes off the intake valve. The parcel distributions in Figure 7 show that some of the splashed parcels form films on the head and intake side of the liner after secondary collisions. Rebound and separation each account for less than 5% of the injected fuel. The integrated model, however, predicts much less splashing and film formation but significantly higher amounts of film separation. It is hypothesized that the new splash criteria used in the integrated model predict less

splashing of fuel off the valve resulting in creation of a film which is then immediately separated from the sharp corners of the valve. It is not possible to test this hypothesis without further information for each collision result.

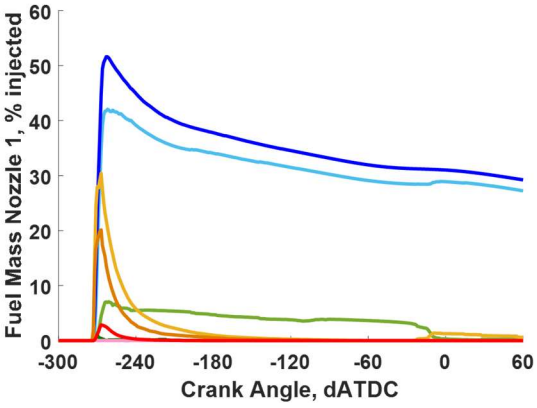

a) Nozzle 1

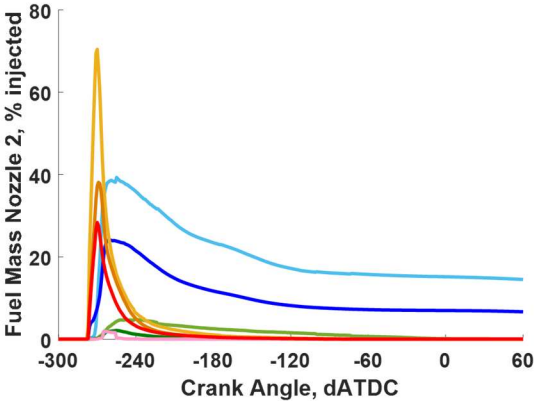

b) Nozzle 2

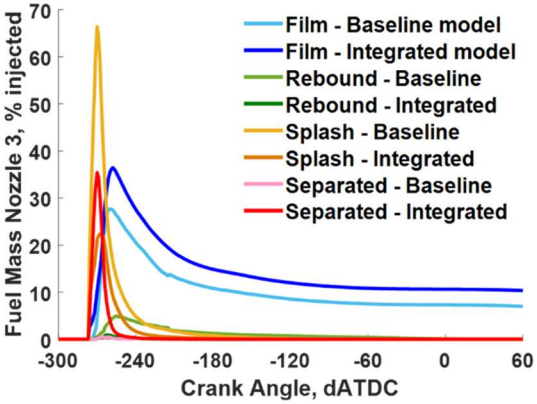

c) Nozzle 3

FIGURE 6: Percent of injected fuel mass for each nozzle grouped by outcome of wall collision predicted by two modeling approaches.

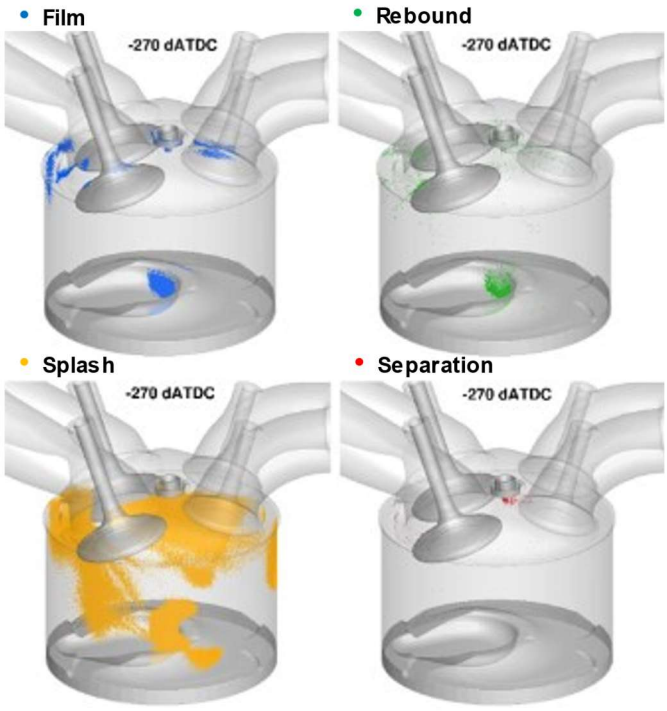

a) Baseline Model

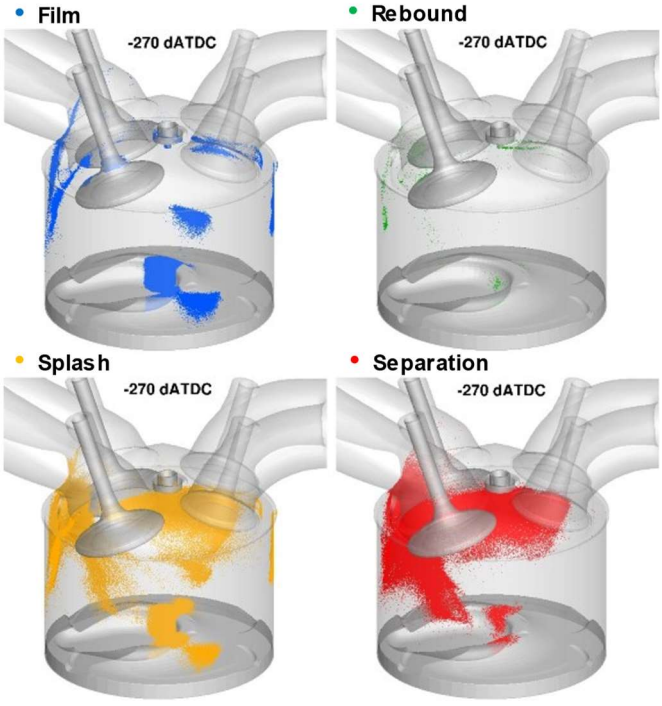

b) Integrated Model

FIGURE 7: Predicted spray distribution based on wall collision outcome 10 CAD after start of injection as predicted by two modeling approaches.

The portion of the spray plume from Nozzle 2 which does not impact the valve continues across the cylinder and impacts the liner. In the baseline model, almost all of these parcels either splash or rebound off the liner, whereas the integrated model predicts significant film formation on the liner.

Similarly, the baseline model predicts that fuel from Nozzle 3 which impacts the intake valve is mostly splashed with a small amount of film formed on the intake valve. Again, the integrated model predicts much less splashing and more separation from the collisions with the intake valve. In both models, many of the splashed and/or separated fuel parcels maintain forward momentum eventually having secondary wall collisions and forming a significant amount of film on the spark plug, head, exhaust valves, and liner. The remainder are either deflected upward impacting the head or backward impacting the intake side of the engine.

The portion of fuel spray from Nozzle 3 which does not impact the intake valve continues unimpeded until it hits the liner on the exhaust side of the cylinder ahead of the splashed/separated fuel parcels that hit the intake valve. The baseline model predicts the free spray splashes off the liner with no film being formed here until the secondary impact of splashed parcels. The integrated model, however, predicts substantial film formation from the free spray impact.

Due to the limited availability of experimental spray measurements for the stock injector, it is unknown if the predicted spray patterns accurately capture actual spray behavior at these conditions. (Prior to the early end of the PACE program, efforts had been planned to address these data needs with additional spray-chamber experiments.) However, the trends observed over a start-of-injection (SOI) sweep match trends observed in experimental measurements of soot and fuel loss (injected mass vs. emissions-based C balance). For earlier SOI, the CFD model predicts less valve interaction with significant increases in spray penetration and wall wetting/pooling on the piston. With the earlier timing, Nozzle 2 also hits the piston instead of the liner further contributing to pooling on the piston face. Experiments at the same conditions show dramatic increases in soot production (possibly from pool burning on the piston) and increased fuel loss. For later SOI, the CFD model predicts more valve interaction with increases in film formation on the head, liner, and intake port and significant reductions in pooling on the piston. This also matches experimental observations of increased fuel loss for SOI later than −280 dATDC but reduced soot emissions (potentially due to less pool burning on the piston).

4. CONCLUSION

A summary of key learnings and conclusions from this numerical study of in-cylinder fuel injection at cold start–relevant conditions follows:

- Film composition differs considerably from the injection surrogate formulation due to preferential evaporation of the lighter fuel species.
- Significant differences in spray–wall collision outcomes and location of film formation within the cylinder are noted for the two modeling approaches.
- Despite these differences, only a small increase in initial total film mass is predicted by the integrated model with the additional mass dissipating quickly during the intake stroke and film mass converging toward that predicted by the baseline model.

ACKNOWLEDGEMENTS

The author would like to acknowledge support for this work under the PACE consortium from the U.S. DOE Vehicle Technologies Office program and technology managers Gurpreet Singh and Michael Weismiller.

The author would like to acknowledge efforts of the PACE team including Roberto Torelli, Tuan Nguyen, et al. for development of the PACE spray submodels, Scott Wagnon for development of the PACE-20 fuel surrogate, and Jatana Gurneesh for cold-start experimental efforts on the GM LNF engine. The author would also like to acknowledge Convergent Science, Inc. for licenses and support for CONVERGE v3.0.

This manuscript has been authored by UT-Battelle, LLC, under contract DE-AC05-00OR22725 with the US Department of Energy (DOE).

Portions of this research used resources of the Compute and Data Environment for Science (CADES) at the Oak Ridge National Laboratory, which is supported by the Office of Science of the U.S. Department of Energy under Contract No. DE-AC05-00OR22725.

REFERENCES

[1] J Rodriguez, W Cheng (2017). “Analysis of NOx emissions during crank-start and cold fast-idle in a GDI engine”. *SAE International Journal of Engines* 10(2):646–655 (*SAE technical paper 2017-01-0796*). doi:10.4271/2017-01-0796.

[2] PJ O’Rourke, AA Amsden (2000). “A spray/wall interaction submodel for the KIVA-3 wall film model”. *SAE technical paper 2000-01-0271*. doi:10.4271/2000-01-0271.

[3] C Mundo, M Sommerfeld, C Tropea (1995). “Droplet-wall collisions: Experimental studies of the deformation and breakup process”. *International Journal of Multiphase Flow* 21(2):151–173. doi:10.1016/0301-9322(94)00069-V.

[4] TM Nguyen, RN Dahms, LM Pickett, F Tagliante (2022). “The Corrected Distortion model for Lagrangian spray simulation of transcritical fuel injection”. *International Journal of Multiphase Flow* 148:103927. doi: 10.1016/j.ijmultiphaseflow.2021.103927.

[5] R Torelli, R Scarcelli, S Som, X Zhu, SY Lee, J Naber, D Markt, M Raessi (2022). “Toward predictive and computationally affordable Lagrangian–Eulerian modeling of spray–wall interaction”. *International Journal of Engine Research* 21(2). doi:10.1177/1468087419870619.

[6] Convergent Science, Inc. (2020). *CONVERGE v3.0 manual*.

[7] C Price, A Hamzehloo, P Aleiferis, R Richardson (2016). “An approach to modeling flash-boiling fuel sprays for direct-

injection spark-ignition engines." *Atomization and Sprays* 26(12):1197–1239. doi:10.1615/AtomizSpr.2016015807.

[8] DW Stanton, CJ Rutland (1996). "Modeling fuel film formation and wall interaction in diesel engines". *SAE technical paper 960628*. doi:10.4271/960628.

[9] DW Stanton, CJ Rutland (1998). "Multi-dimensional modeling of heat and mass transfer of fuel films resulting from impinging sprays". SAE technical paper 980132. doi:10.4271/980132.

[10] DW Stanton, CJ Rutland (1998). "Multi-dimensional modeling of thin liquid films and spray–wall interactions resulting from impinging sprays". *International Journal of Heat and Mass Transfer* 41(20):3037–3054. doi:10.1016/S0017-9310(98)00054-4.